

Towards efficient and universal entanglement detection

Jue Xu* and Qi Zhao†

(Dated: August 22, 2022)

Verification (detection) of entanglement structure is an indispensable step for practical quantum computation (communication). In this work, we compare complexity and performance of several recently-developed methods, including entanglement witness methods, shadow tomography, classical machine learning, and quantum algorithms (circuits). We illustrate the advantages and limitations of machine learning and quantum algorithms.

CONTENTS

I. Introduction	1
II. Preliminaries	2
A. Notations	2
B. Entanglement structures	2
C. Entanglement detection	7
D. Tomography and trace estimation	9
III. Classical, data-powered, and quantum algorithms	10
A. Classical shadow and machine learning	11
B. Quantum trace (kernel) estimation	13
C. Variational (hybrid) quantum algorithms	15
D. Theoretic upper bounds and lower bounds	16
IV. Numerical simulation	17
A. Classification accuracy	17
B. Robustness to noise	17
C. Experiments	18
V. Conclusion and discussion	18
Acknowledgements	18
References	18
A. Machine learning background	19
1. Support vector machine	19
2. Neural network	20
B. Hardness assumptions	20

I. INTRODUCTION

Entanglement [1] is the key ingredient of quantum computation [], quantum communication [], and quantum cryptography []. For practical purpose, it is essential to benchmark (characterize) multipartite entanglement structures of target states. We review the recently developed methods to entanglement detection: entanglement witness [2], shadow tomography [3], classical machine learning [4], and quantum (variational/circuit) algorithms [5].

* juexu@cs.umd.edu

† email

II. PRELIMINARIES

A. Notations

Notations: The hats on the matrices such as \hat{A} , \hat{H} , ρ (omitted), \hat{O} , \hat{W} , emphasize that they play the roles of operators (Hermitian matrices). Denote vector (matrix) \mathbf{x} , \mathbf{K} by boldface font. A simple (undirected, unweighted) graph $G = (V, E)$ is described by vertices V and edges E .

For specific purpose, we use different basis (representations) for quantum states. One is the computational basis $\{|z\rangle\}$ with $z \in [2^n]$ where n is the number of qubits, while another useful one is the binary representation of computational basis $\{|\mathbf{x}\rangle \equiv |x_1\rangle |x_2\rangle \dots |x_n\rangle\}$ with $x_j \in \{0, 1\}$. For simplicity, we let $N \equiv 2^n$ and $|\mathbf{0}\rangle \equiv |0^n\rangle \equiv |0\rangle^{\otimes n}$ if no ambiguity. shorthand $|\psi_A\rangle |\psi_B\rangle \equiv |\psi_A\rangle \otimes |\psi_B\rangle$ (we omitted the tensor product for readability). Hadamard basis $|+\rangle := (|0\rangle + |1\rangle)/\sqrt{2}$.

Definition 1 (density matrix). pure state $|\psi\rangle$; A quantum state ρ is defined to be a positive operator $\rho \in \text{End}(V)$ with $\text{Tr}(\rho) = 1$. density matrix ρ (trace one, Hermitian, PSD)...

Definition 2 (POVM). A positive-operator valued measurement (POVM) M consists of a set of positive operators that sum to the identity operator $\mathbf{1}$. When a measurement $M = \{E_1, \dots, E_k\}$ is applied to a quantum state ρ , the outcome is $i \in [k]$ with probability $p_i = \text{tr}(\rho E_i)$. observables ... $\mathbb{E}[x] \equiv \langle \hat{O}_x \rangle := \text{tr}(\hat{O}_x \rho)$

Definition 3 (positive, semidefinite). denoted $X \preceq Y$ provided $Y - X$ is positive

Definition 4 (partial trace). reduced density matrix $\rho_A = \text{Tr}_B(\rho_{AB})$

1. Distance measures

Definition 5 (fidelity). Given a pair of states (target ρ and prepared ρ'), Uhlmann fidelity $F(\rho, \rho') := \text{Tr}(\sqrt{\sqrt{\rho}\rho'\sqrt{\rho}}) \equiv \|\sqrt{\rho}\sqrt{\rho'}\|_1$, where $\sqrt{\rho}$ denotes the positive semidefinite square root of the operator ρ . (infidelity $1 - F(\rho, \rho')$) For any mixed state ρ and pure state $|\psi\rangle$, $F(\rho, |\psi\rangle\langle\psi|) = \sqrt{\langle\psi|\rho|\psi\rangle} \equiv \sqrt{\text{Tr}(\rho|\psi\rangle\langle\psi|)}$ which can be obtained by the Swap-test[?]. linear fidelity or overlap $F(\rho, \rho') := \text{tr}(\rho\rho')$.

different distance measures [6]

Definition 6 (norm). Schatten p-norm $\|x\|_p := (\sum_i |x_i|^p)^{1/p}$. Euclidean norm l_2 norm; Spectral (operator) norm $\|\mathbf{x}\|_\infty$; Trace norm $\|A\|_{\text{Tr}} \equiv \|A\|_1 := \text{Tr}(|A|) \equiv \text{Tr}(\sqrt{A^\dagger A})$, $|A| := \sqrt{A^\dagger A}$, $p = 1$; Frobenius norm $\|A\|_F := \sqrt{\text{Tr}(A^\dagger A)}$, $p = 2$; Hilbert-Schmidt norm $\|A\|_{HS} := \sqrt{\sum_{i,j} A_{ij}^2} = \sqrt{\sum_{i \in I} \|Ae_i\|_H^2}$; Hilbert-Schmidt inner product $\langle A, B \rangle_{\text{HS}} := \text{Tr}(A^\dagger B)$, Frobenius inner product $\langle A, B \rangle_F := \text{Tr}(A^\dagger B)$? (in finite-dimensional Euclidean space, the HS norm is identical to the Frobenius norm) Although the Hilbert-Schmidt distance is arguably not too meaningful, operationally, one can use Cauchy-Schwarz to relate it to the very natural trace distance.

Definition 7 (distance). For mixed states, trace distance $d_{\text{tr}}(\rho, \rho') := \frac{1}{2}\|\rho - \rho'\|_1$. For pure states, $d_{\text{tr}}(|\psi\rangle, |\psi'\rangle) := \frac{1}{2}\| |\psi\rangle\langle\psi| - |\psi'\rangle\langle\psi'| \|_1 = \sqrt{1 - |\langle\psi|\psi'\rangle|^2}$. fidelity and trace distance are related by the inequalities

$$1 - F \leq D_{\text{tr}}(\rho, \rho') \leq \sqrt{1 - F^2} \quad (1)$$

variation distance of two distribution $d_{\text{var}}(p, p') := \frac{1}{2} \sum_i |p_i - p'_i| = \frac{1}{2}\|p - p'\|_1$. l_2 distance ... Hellinger distance ... HS distance $D_{\text{HS}}(\rho, \rho') := \|\rho - \rho'\|_{\text{HS}} = \sqrt{\text{Tr}((\rho - \rho')^2)}$

B. Entanglement structures

1. Bipartite entanglement

Large scale entanglement is the (main) resource of quantum advantages in quantum computation and communication. Firstly, we consider the simplest entanglement structure: bipartite separable case. Many methods [...] have been developed to determine whether a state is separable.

Definition 8 (bipartite separable). A pure state is (bi-)separable if it is in a tensor product form $|\psi_b\rangle = |\phi_A\rangle \otimes |\phi_{\bar{A}}\rangle$, where $\mathcal{P}_2 = \{A, \bar{A}\}$ is a bipartition of the qubits in the system. Note that the state $|\phi_A\rangle$ may be entangled, thus the state $|\psi\rangle$ is not necessarily **fully separable**. A mixed state is separable iff it can be written as a convex combination of pure biseparable states $\rho = \sum_i p_i |\psi_i\rangle\langle\psi_i|$ where $|\psi_i\rangle$ may be biseparable with respect to different partitions (otherwise **genuine multipartite entanglement**). The simple statement “The state is entangled” would still allow that only two of the qubits are entangled while the rest is in a product state.

Consider a bipartite system AB with the Hilbert space $\mathcal{H}_A \otimes \mathcal{H}_B$, where \mathcal{H}_A has dimension d_A and \mathcal{H}_B has dimension d_B , respectively. A state ρ_{AB} is *separable* if it can be written as a convex combination $\rho_{AB} = \sum_i \lambda_i \rho_{A,i} \otimes \rho_{B,i}$ with a probability distribution $\lambda_i \geq 0$ and $\sum_i \lambda_i = 1$. Otherwise, ρ_{AB} is entangled.

Note that each separable state $|\psi_b\rangle$ in the summation can have different bipartitions. The separable state set is denoted as S_b . There is another restricted way for the extension to mixed states. A state is \mathcal{P}_2 -separable, if it is a mixing of pure separable states with a same partition \mathcal{P}_2 , and we denote the state set as $S_b^{\mathcal{P}_2}$. entangled state?...

Rather than qualitatively determining (bi)separability, there are measures to quantify entanglement

Definition 9 (Schmidt measure). Consider the following bipartite pure state, written in Schmidt form:

$$|\psi\rangle = \sum_i^r \sqrt{p_i} |\phi_i^A\rangle \otimes |\phi_i^B\rangle \quad (2)$$

where $\{|\phi_i^A\rangle\}$ is a basis for \mathcal{H}_A and $\{|\phi_i^B\rangle\}$ for \mathcal{H}_B . The strictly positive values $\sqrt{p_i}$ in the Schmidt decomposition are its *Schmidt coefficients*. The number of Schmidt coefficients, counted with multiplicity, is called its *Schmidt rank*, or Schmidt number. (Schmidt rank ?? $\text{SR}^A(\psi) = \text{rank}(\rho_\psi^A)$) Schmidt measure is minimum of $\log_2 r$ where r is number of terms in an expansion of the state in product basis.

Definition 10 (entropy). In quantum mechanics (information), the von Neumann *entropy* of a density matrix is $H_N(\rho) := -\text{Tr}(\rho \log \rho) = -\sum_i \lambda_i \log(\lambda_i)$; In classical information (statistical) theory, the Shannon entropy of a probability distribution P is $H_S(P) := -\sum_i P(x_i) \log P(x_i)$. relative entropy (**divergence**)

Remark 1. a pure (bipartite) state is entangled iff the reduced state $\rho^A = \text{Tr}_B(\rho)$ is mixed. The mixedness of this reduced state allows one to quantify the amount of entanglement in this state.

Definition 11 (entanglement entropy). The bipartite *von Neumann entanglement entropy* S is defined as the von Neumann entropy of either of its reduced density matrix ρ_A . For a pure state $\rho_{AB} = |\Psi\rangle\langle\Psi|_{AB}$, it is given by

$$E(\Psi_{AB}) = S(\rho_A) = -\text{Tr}(\rho_A \log \rho_A) = -\text{Tr}(\rho_B \log \rho_B) = S(\rho_B) \quad (3)$$

where $\rho_A = \text{Tr}_B(\rho_{AB})$ and $\rho_B = \text{Tr}_A(\rho_{AB})$ are the reduced density matrices for each partition. With Schmidt decomposition (Eq. (2)), the entropy of entanglement is simply $-\sum_i p_i^2 \log(p_i)$. the n th Renyi entropy, $S_n = \frac{1}{n-1} \log(R_n)$ where $R_n = \text{Tr}(\rho_A^n)$

Definition 12 (maximally entangled). a state vector is *maximally entangled* iff the reduced state at one qubit is maximally mixed, i.e., $\text{Tr}_A(|\psi\rangle\langle\psi|) = \frac{1}{2}$.

Classically, the hardness of determining the bipartite separability.

Theorem 1 ([7]). *The weak membership problem for the convex set of separable normalized bipartite density matrices is NP-Hard. Input: unknown state?? formal definition of the problem [8]*

However, we do not know approximately correct complexity? quantum complexity? machine learning (data)? for entanglement () problem? multipartite?

Definition 13 (partial transpose). [9] The partial transpose (PT) operation - acting on subsystem A - is defined as

$$|k_A, k_B\rangle\langle l_A, l_B|^{\tau_A} := |l_A, k_B\rangle\langle k_A, l_B| \quad (4)$$

where $\{|k_A, k_B\rangle\}$ is a product basis of the joint system AB .

The well-known PPT condition checks if the partially transposed (PT) density matrix $\rho_{AB}^{\tau_A}$ is **positive, semidefinite**. If the PPT condition is violated - i.e. $\rho_{AB}^{\tau_A}$ does have negative eigenvalues - A and B must be entangled.

Theorem 2 (PPT criterion). [9] *the positive partial transpose (PPT) criterion, saying that a separable state (bipartite separable) must have PPT?. Note, it is only necessary and sufficient when $d_A d_B \leq 6$. Another widely used one is the k -symmetric extension hierarchy [15, 16], which is presently one of the most powerful criteria, but hard to compute in practice due to its exponentially growing complexity with k .[??]*

However, up to now, no general solution for the separability problem is known. Similar to the PPT condition, the p_3 -PPT condition applies to mixed states and is completely independent of the state in question. This is a key distinction from entanglement witnesses, which can be more powerful, but which **usually require detailed prior information about the state**. From this data set, the PT-moments p_n can be estimated without having to reconstruct the density matrix ρ_{AB} , and with a significantly smaller number of experimental runs M than required for full quantum state tomography. c.f. [5], [entanglement spectroscopy](#)

2. Multipartite entanglement structures

For multipartite quantum systems, it is crucial to identify not only the presence of entanglement but also its detailed structure. An identification of the entanglement structure may thus provide us with a hint about where imperfections in the setup may occur, as well as where we can identify groups of subsystems that can still exhibit strong quantum-information processing capabilities.

Given a n -qubit quantum system and its partition into m subsystems, the *entanglement structure* indicates how the subsystems are entangled with each other. In some specific systems, such as distributed quantum computing[] quantum networks[] or atoms in a lattice, the geometric configuration can naturally determine the system partition. Therefore, it is practically interesting to study entanglement structure under partitions.

Definition 14 (fully entangled). An n -qubit quantum state ρ is a *fully entangled*, if it is outside of the separable state set $S_b^{P_2}$ for any partition, $\rho \notin S_b^{P_2}, \forall P_2 = \{A, \bar{A}\}$.

GME is the strongest form of entanglement, that is, all qubits in the system are indeed entangled with each other. The size of the genuinely entangled quantum system becomes a figure of merit for assessing the advancement of quantum devices in the competition among various realizations.

Definition 15 (genuine multipartite entanglement). A state possesses *genuine multipartite entanglement* (GME) if it is outside of S_2 , and is (fully) n -separable if it is in S_n . A state possesses \mathcal{P} -genuine entanglement if it is outside of $S_b^{\mathcal{P}}$. A state ρ possesses \mathcal{P} -genuine entanglement iff $\rho \notin S_b^{\mathcal{P}}$.

Compared with genuine entanglement, multipartite entanglement structure still lacks a systematic exploration, due to the rich and complex structures of n -partite system. Unfortunately, it remains an open problem of efficient entanglement-structure detection of general multipartite quantum states.

Definition 16 (Multipartite state). denote the partition $\mathcal{P}_m = \{A_i\}$ and omit the index m when it is clear from the context.

define fully- and biseparable states with respect to a *specific partition* \mathcal{P}_m

Definition 17 (fully separable). An n -qubit pure state $|\psi_f\rangle$ is *fully separable* iff. An n -qubit pure state $|\psi_f\rangle$ is \mathcal{P} -fully separable iff it can be written as $|\psi_f\rangle = \otimes_i^m |\phi_{A_i}\rangle$. An n -qubit mixed state ρ_f is \mathcal{P} -fully separable iff it can be decomposed into a convex mixture of \mathcal{P} -fully separable pure states.

$$\rho_f = \sum_i p_i |\psi_f^i\rangle\langle\psi_f^i|, (\forall i)(p_i \geq 0, \sum_i p_i = 1). \quad (5)$$

P-bi-separable... $S_f^{\mathcal{P}} \subset S_b^{\mathcal{P}}$

By going through all possible partitions, one can investigate higher level entanglement structures, such as entanglement intactness (non-separability), which quantifies how many pieces in the n -partite state are separated.

Remark 2. P-... can be viewed as generalized versions of regular fully separable, biseparable, and genuinely entangled states, respectively. In fact, when $m = n$, these pairs of definitions are the same. By definitions, one can see that if a state is \mathcal{P}_m -fully separable, it must be m -separable. Of course, an m -separable state might not be \mathcal{P}_m -fully separable, for example, if the partition is not properly chosen.

entanglement structure measures. To benchmark our technological progress towards the generation of largescale genuine multipartite entanglement, it is thus essential to determine the corresponding entanglement depth.

Definition 18 (Entanglement intactness, depth). the entanglement intactness of a state ρ to be m , iff $\rho \notin S_{m+1}$ and $\rho \in S_m$. When the entanglement intactness is 1, the state possesses [genuine multipartite entanglement](#); and when the intactness is n , the state is [fully separable](#). k -producible.

Example 1. The **Schmidt measure** for any multi-partite **GHZ** states is 1, because there are just two terms. Schmidt measure for 1D, 2D, 3D-cluster state is $\lfloor \frac{N}{2} \rfloor$. Schmidt measure of tree is the size of its minimal vertex cover[??].

Example 2 (GHZ). bipartite: Bell states; nontrivial multipartite: tripartite. Greenberger-Horne-Zeilinger (GHZ) state: $|\text{GHZ}\rangle := \frac{1}{\sqrt{2}}(|0\rangle^{\otimes n} + |1\rangle^{\otimes n})$ (eight-photon) produce the five different entangled states (one from each entanglement structure/partition?):

$$|\text{GHZ}_8\rangle, |\text{GHZ}_{62}\rangle, |\text{GHZ}_{44}\rangle, |\text{GHZ}_{422}\rangle, |\text{GHZ}_{2222}\rangle.$$

The GHZ-state is generally considered as the state with the genuine 3partite entanglement, while the W-state has the peculiar property of having the maximal expected amount of two-partite entanglement if one party is traced out. Schmidt rank, PPT criteria, entanglement witness...

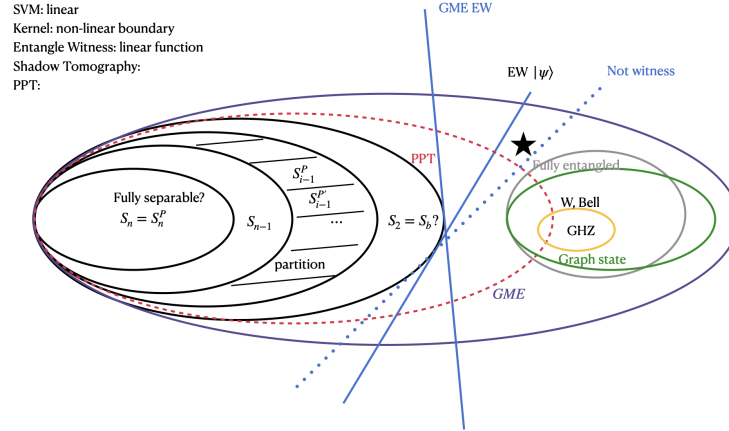


FIG. 1: (a) **entanglement witness**, **PPT criterion**, **SVM** (kernel)?. convex hull...

3. Graph state

graph state is an important (large?) class of multipartite states in quantum information. Typical graph states include cluster (lattice) states, **GHZ** states, and the states involved in error correction (toric code?). It worth noting that 2D cluster state is the universal resource for the measurement based quantum computation (MBQC) [10].

Definition 19 (graph state). Given a simple graph (undirected, unweighted, no loop and multiple edge) $G = (V, E)$, a graph state is constructed as from the initial state $|+\rangle^{\otimes n}$ corresponding to n vertices. Then, apply controlled-Z gate to every edge, that is

$$|G\rangle := \prod_{(i,j) \in E} cZ_{(i,j)} |+\rangle^{\otimes n} \quad (6)$$

Remark 3. An n -partite(qubit) graph state can also be uniquely determined by n independent stabilizers, $S_i := X_i \otimes_{j \in n} Z_j$, which commute with each other and $\forall i, S_i |G\rangle = |G\rangle$.?? The graph state is the unique eigenstate with eigenvalue of +1 for all the n stabilizers. As a result, a graph state can be written as a product of stabilizer projectors, $|G\rangle\langle G| = \prod_{i=1}^n \frac{S_i + 1}{2}$. stabilizer formalism ?;

Example 3 (graph states). Any connected graph state is **fully entangled** state. The **GHZ** state corresponds to the star graph and the complete graph (Fig. 2). This is easily seen by applying Hadamard unitaries $\hat{U}_H^{V \setminus a}$ to all but one qubit a in the GHZ-state, which yields the star graph state with a as the central qubit. (line, ring; hypercube, Petersen graph; cluster state in two dimensions, which corresponds to a rectangular lattice.) The Petersen graph is not LC-equivalent to its isomorphism (exchanging the labels at each edge of the five “spokes”). However, the lists of Schmidt ranks (or, equivalently, the connectivity functions) of these graphs coincide. The class of CSS (error correction) states corresponds to the class of 2-colorable graphs. [11]

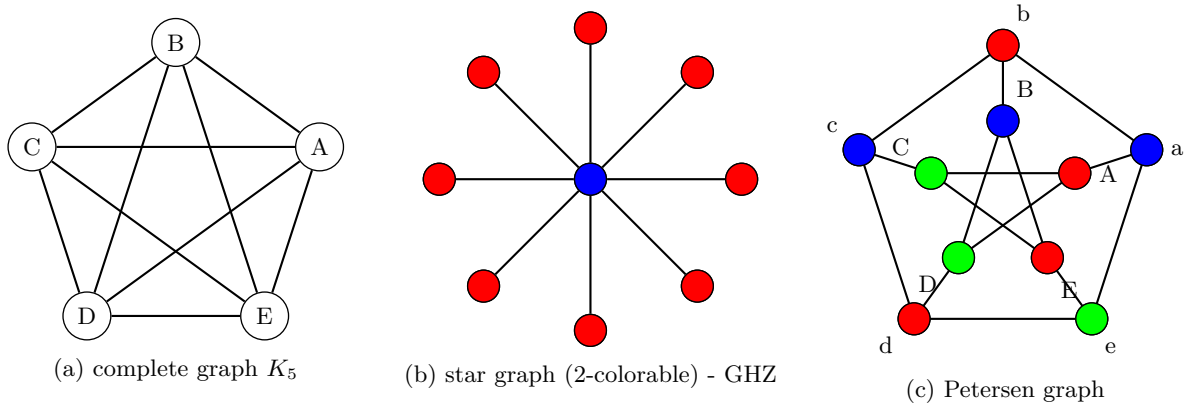


FIG. 2: graph states

Remark 4 (??). The entanglement [entropy](#) $S(\rho_A)$ equals the rank of the adjacency matrix of the underlying bipartite graph, which can be efficiently calculated. For graph states, the reduced density matrices can be represented efficiently in terms of their stabilizer elements or their adjacency matrix.

Proposition 1 ([2]). Given a graph state $|G\rangle$ and a partition $\mathcal{P} = \{A_i\}$, the [fidelity](#) between $|G\rangle$ and any [fully separable](#) is upper bounded by

$$\text{Tr}(|G\rangle\langle G| \rho_f) \leq \min_{\{A, \bar{A}\}} 2^{-S(\rho_A)} \quad (7)$$

where $S(\rho_A)$ is the von Neumann [entropy](#) of the reduced density matrix $\rho_A = \text{Tr}_{\bar{A}}(|G\rangle\langle G|)$.

Remark 5. LU, LC equivalence, local operations and classical communication (LOCC)

the entanglement in a graph state is related to the topology of its underlying graph.

Proposition 2 (Entanglement of graph state). [11]. [witness](#); [bounds](#); [graph property](#)? [vertex cover](#)? [Hamiltonian cycle](#) of a graph state?

generalize [12] stabilizer state, neural network state [13]?

Proposition 3 (Entanglement witness for graph state). [Bell inequality](#)

$$\hat{W} = \frac{C}{2^N} \mathbb{1}_V - |G\rangle\langle G| \quad (8)$$

Let $|G\rangle$ be a graph state corresponding to a connected graph. Then

$$\hat{W}_1^{ab} = \mathbb{1}_V - K_a - K_b \quad (9)$$

is an entanglement witness for the $|G\rangle$ that detects entanglement in the reduced state $\rho_G^A (A = N_a \cup N_b \cup \{a, b\})$ with only two measurement settings and thus can rule out full separability of the total graph state???. The entanglement witness

$$\hat{W}_2 = (N - 1) \mathbb{1}_V - \sum_{a \in V} K_a \quad (10)$$

detects [genuine multipartite entanglement](#).

Question 1. for which case, C is hard to compute? non-stabilizer state? SWAP?

Theorem 3. k local measurements. Here, k is the chromatic number (minimal [colorable](#)) of the corresponding graph, typically, a small constant independent of the number of qubits.

200 **Theorem 4.** [14]

$$\max_{\rho \in SEP} \sum_{i=1}^n \langle A_i \otimes B_i \rangle \leq \sqrt{\theta(\bar{G}_A)\theta(\bar{G}_B)} =: \theta_{AB} \quad (11)$$

201 where $\theta(\bar{G}_A)$ is the Lovasz number of the anticommutativity graph of $\{A_i\}$ and similarly for $\theta(\bar{G}_B)$. This separability
202 criterion naturally leads to entanglement witnesses of the form

$$\hat{W}_{\mathbb{E}} = \theta_{AB} \mathbb{1} - \sum_i A_i \otimes B_i \quad (12)$$

203 **Proposition 4** (Bounds to the Schmidt measure of graph states). For any graph state $|G\rangle$, the *Schmidt measure*
204 E_A is bounded from below by the maximal Schmidt rank SR_{\max} and from above by the Pauli persistency PP or the
205 minimal vertex cover, i.e.

$$\text{SR}_{\max}(G) \leq E_S(|G\rangle) \leq \text{PP}(G) \leq \text{VC}(G). \quad (13)$$

206 ???

207

C. Entanglement detection

208 *PPT criterion*

209

1. Entanglement witness

210 see Fig. 1 for relations. entanglement detection [15].

211 **Definition 20** (entanglement witness). Given an (unknown? known target state) quantum state (density matrix) ρ ,
212 the *entanglement witness* \hat{W} is an observable such that

$$\mathbb{E}_{\rho}[\hat{W}] \equiv \langle \hat{W} \rangle \equiv \text{Tr}(\hat{W}\rho) \geq 0, \forall \text{ separable}; \quad \text{Tr}(\hat{W}\rho) < 0, \text{ for some entangled} \quad (14)$$

213 [16], see Fig. 1

214

2. Fidelity, projector-based witness

215 In a typical experiment one aims to prepare a pure state, $|\psi\rangle$, and would like to detect it as true multipartite
216 entangled. While the preparation is never perfect, it is still expected that the prepared mixed state is in the proximity
217 of $|\psi\rangle$. The usual way to construct entanglement witnesses using the knowledge of this state is

$$\hat{W}_{\psi} = c\mathbb{1} - |\psi\rangle\langle\psi| \quad (15)$$

218 where c is the smallest constant such that for every product state $\text{Tr}(\rho\hat{W}) \geq 0$

219 **Proposition 5** (Section 6.3 of [17]). A state ρ is separable iff $\forall \hat{W}, \text{Tr}[\rho\hat{W}] \geq 0$. Corollary, a state ρ is entangled iff
220 $\exists \hat{W}, \text{Tr}[\rho\hat{W}] < 0$. There is no entanglement witness that detects all entangled states.

221 **Remark 6.** In order to measure the witness in an experiment, it must be decomposed into a sum of locally measurable
222 operators. The number of local measurements in these decompositions seems to increase exponentially with the number
223 of qubits.[??]

224 **Example 4** (entanglement witness for GHZ). three-qubit GHZ state [18]

$$\hat{W}_{\text{GHZ}_3} := \frac{3}{2}\mathbb{1} - \hat{\sigma}_x^{(1)}\hat{\sigma}_x^{(2)}\hat{\sigma}_x^{(3)} - \frac{1}{2}\left[\hat{\sigma}_z^{(1)}\hat{\sigma}_z^{(2)} + \hat{\sigma}_z^{(2)}\hat{\sigma}_z^{(3)} + \hat{\sigma}_z^{(1)}\hat{\sigma}_z^{(3)}\right] \quad (16)$$

This witness requires the measurement of the $\{\hat{\sigma}_x^{(1)}, \hat{\sigma}_x^{(2)}, \hat{\sigma}_x^{(3)}\}$ and $\{\hat{\sigma}_z^{(1)}, \hat{\sigma}_z^{(2)}, \hat{\sigma}_z^{(3)}\}$ settings. The projector based witness $\hat{W}_{\text{GHZ}_3} = \mathbb{1}/2 - |\text{GHZ}\rangle\langle\text{GHZ}|$ requires four measurement settings. detect genuine n -qubit entanglement close to GHZ_n

$$\hat{W}_{\text{GHZ}_n} = (n-1)\mathbb{1} - \sum_{k=1}^n S_k^{(\text{GHZ}_n)} \quad (17)$$

\hat{S}_k is the Stabilizer ... [19] Detecting Genuine Multipartite Entanglement with Two Local Measurements [18]

Question 2. how far/close to the target state (entanglement witness), noise limit?

It is natural to ask how nonlinear entanglement witness [20] and the kernel method (nonlinear boundary) in machine learning can be applied.

Proposition 6. Given a state $|\psi\rangle$, the entanglement witness operator \hat{W}_ψ can witness genuine multipartite entanglement near $|\psi\rangle$ with $c = 5/8$ in Eq. (15) that is, $\langle \hat{W}_\psi \rangle \geq 0$ for any separable state in S_b .

If the fidelity (quantum kernel?) of the prepared state ρ_{pre} with the target state $|\psi\rangle$, i.e., $\text{Tr}(\rho_{\text{pre}} |\psi\rangle\langle\psi|)$, exceeds $5/8$, ρ_{pre} possesses GME. It is generally difficult to evaluate the quantity $\text{Tr}(\rho_{\text{pre}} |\psi\rangle\langle\psi|)$ by the direct projection on $|\psi\rangle$, as it is an entangled state.

	$ \text{GHZ}_3\rangle$	$ W_3\rangle$	$ CL_3\rangle$	$ \psi_2\rangle$	$ \mathcal{D}_{2,4}\rangle$	$ \text{GHZ}_n\rangle$	$ W_3\rangle$	$ G_n\rangle$
α	1/2	2/3	1/2	3/4	2/3	1/2	$(n-1)/n$	1/2
maximal p_{noise}	4/7	8/21	8/15	4/15	16/45	$1/2 \cdot (1 - 1/2^n)^{-1}$		
local measurements	4	5	9	15	21	N+1	$2N-1$	depend on graphs

TABLE I: [15]

For non-stabilizer case, [12] [21]

3. Bell inequality witness

A usual approach for detecting entanglement is using Bell inequalities [??]

Definition 21 (Bell inequality).

$$a_0 = \hat{\sigma}_z, a'_0 = \hat{\sigma}_x, b_0 = (\hat{\sigma}_x - \hat{\sigma}_z)/\sqrt{2}, b'_0 = (\hat{\sigma}_x + \hat{\sigma}_z)/\sqrt{2}, \mathbf{w} = \{\pm 2, 1, -1, 1, 1\} \quad (18)$$

Bell inequalities for graph states $|\sum_{\sigma \in S} \langle \sigma \rangle| \leq C? \dots$

Definition 22 (CHSH inequality). CHSH inequality (game) ...;

$$\{a_0 b_0, a_0 b'_0, a'_0 b_0, a'_0 b'_0\} \quad (19)$$

Remark 7. However, even for two-qubit systems there exist entangled states which do not violate any Bell inequality. Bell inequalities are not suited to this aim in general. Multiseparable and biseparable states violate known Bell inequalities less than n -partite Greenberger-Horne-Zeilinger (GHZ) states. However, for $n > 3$ there exist even pure n -partite entangled states with a lower violation than biseparable states. [22]

Example 5 (inequality). [23] First, there exist entangled states not violating the Bell inequalities. To be more specific, the maximally-entangled state, such as $|\psi_0\rangle = (|00\rangle - |11\rangle)/\sqrt{2}$ for a pair of qubits, can maximally violate the CHSH inequality. However, this tool fails under the circumstances of noise, in the form of a quantum channel. After passing through a depolarizing channel, the resulting state,

$$\rho = p |\psi_0\rangle\langle\psi_0| + (1-p) \frac{\mathbb{1}}{4} \quad (20)$$

where $0 \leq p \leq 1$, violates the CHSH inequality only if $p > 1/\sqrt{2}$. However, the state is entangled when $p > 1/3$.

Another approach for detecting multipartite entanglement is using entanglement witnesses. Different Bell inequalities can be regarded as entanglement witness for different types of entanglement in a multi-party entangled state. These witnesses can be quite useful to detect entanglement in the vicinity of graph states.

Problem 1 (separability). given (input) an **unknown** state, to determine (output) separability.

Problem 2 (Entanglement witness with prior). Entanglement witness

- **Input:** a **known** state $|\psi\rangle$, with noise

- **Output:** separable or not ENTANGLED ??? S_f^P ? S_b^P

difficulty: multi(n)-partite, high-dimensional (qudit) [24], pure/mixed state, with/out prior knowledge, universal?, non-stabilizer [19], certain partition

Remark 8 (universal entanglement witness). [24] For example, a witness specifically designed for a four-qubit compact cluster state [16] confirms, when its expectation value is negative, the presence of that particular state having a very specific density function, while a positive measured expectation value of that operator only provides information that the tested state is not a compact cluster state. Indeed, the same witness, if applied to a four-qubit linear cluster or GHZ [17] states, would result in a positive measured expectation value, even though these two states are both highly entangled [17, 18]. Hence, a witness is a threshold test that can only detect the presence of a specific state. In contrast to an entanglement monotone (e.g. the entanglement entropy [6]), which determines the amount of entanglement, a witness cannot be used to quantify entanglement.

Problem 3 (Certify entanglement). Multipartite entanglement-structure detection

- **Input:** an (actual) state ρ' from experiment that is close to a **known/target** (general multipartite) state $|\psi\rangle$, certain partition?

- **Output:** the certified lower-order entanglement among several subsystems could be still useful for some quantum information tasks. entanglement structure

D. Tomography and trace estimation

The brute force approach is to fully characterize a system by performing quantum state tomography and calculating separability measures from the recovered density matrix. Intuitively, a general tomography [25] that extract (recover) all information of a state requires exponential copies (samples/measurements).

Problem 4 (full tomography). In contrast to **shadow tomography**, we refer to *full tomography* here

- **Input:** Given a **unknown** N -dimensional mixed state ρ

- **Output:** a complete description? of ρ (decomposition coefficients) with error? Stokes parameter $S_i \equiv \text{Tr}(\hat{\sigma}_i \rho)$

$$\rho = \frac{1}{2^n} \sum_{i_1, i_2, \dots, i_n=0}^3 S_{i_1, i_2, \dots, i_n} \hat{\sigma}_{i_1} \otimes \hat{\sigma}_{i_2} \otimes \dots \otimes \hat{\sigma}_{i_n} \quad (21)$$

However, tomography is experimentally and computationally demanding; for a state consisting of N particles, with each residing in a d -dimensional Hilbert space, we would have to perform $M = \mathcal{O}(d^{2N})$ measurements.

Theorem 5 (lower bound of **full tomography**?[26]). *Known fundamental lower bounds [66, 73] state that classical shadows of exponential size (at least) $T = \Omega(2^n/\epsilon^2)$ are required to ϵ -approximate ρ in trace distance.*

In quantum mechanics, interesting properties are often linear functions of the underlying density matrix ρ . For example, the fidelity with a pure target state, entanglement witnesses fit this framework.

Problem 5 (trace estimation). related problems defined as follows

- **Input:** Given an observable (Hermitian) \hat{O} and (copies of) a mixed state ρ or several states (ρ', \dots, ρ_m) ,

- **Output:** with error ϵ measured by trace distance (fidelity...)

- linear function (mostly): the expectation value $\langle \hat{O} \rangle = \text{Tr}(\hat{O}\rho)$; **entanglement witness** $\text{Tr}(\hat{W}\rho)$; **shadow tomography** $\text{Tr}(E_M\rho) = \mathbb{E}[E_M] = \mathbb{P}[E_i \text{ accept } \rho]$??; **full tomography**; $\text{Tr}(\hat{O}\mathcal{E}(|\psi\rangle\langle\psi|))$ where \mathcal{E} is a CPTP (completely positive and trace preserving) map two-point correlation $\langle O_i O_j \rangle$
- nonlinear function: **entropy** (non-linear); quadratic $\text{Tr}(\hat{O}\rho_i \otimes \rho_j)$; **fidelity** $F(\rho, \rho')$, **distance**??;
- multivariate: **quantum kernel** $\text{Tr}(\rho\rho')$; multivariate $\text{Tr}(\rho_1 \cdots \rho_m)$, nonlinear function?? linear;

Nevertheless, we usually only need specific properties of a target state rather than full classical descriptions about the state. This enables the possibility to shadow tomography.

Problem 6 (shadow tomography). *shadow tomography*

- **Input:** an **unknown** N -dimensional mixed state ρ , M known 2-outcome measurements E_1, \dots, E_M
- **Output:** estimate $\mathbb{P}[E_i \text{ accept } \rho]$ to within additive error ϵ , $\forall i \in [M]$, with $\geq 2/3$ success probability.

Theorem 6 (bounds of shadow tomography [27]). *It is possible to do shadow tomography using $\tilde{O}(\frac{\log^4 M \cdot \log N}{\epsilon^4})$ copies. [no construction algorithm?] sample complexity lower bound $\Omega(\log(M) \cdot \epsilon^{-2})$,*

more details in Section III A 1

Remark 9 (compare shadow tomography and classical shadow [3]). While very efficient in terms of samples, Aaronson’s procedure is very demanding in terms of quantum hardware — a concrete implementation of the proposed protocol requires **exponentially long quantum circuits** that act collectively on all the copies of the unknown state stored in a quantum memory??

III. CLASSICAL, DATA-POWERED, AND QUANTUM ALGORITHMS

In this paper, we focus on the entanglement structure detection for graph states.

Problem 7 (detect graph state entanglement structure?). problem without training data

- **Input:** a graph G encoding in a graph state $|G\rangle$; adjacency matrix A ?
- **Output:** entanglement structure??

with training data: **features:** classical shadow? raw data? quantum data, label: entangled?

Definition 23 (input model). several common input (encoding) models in quantum algorithms:

- **amplitude encoding:** given a normalized vector $\mathbf{x} \in \mathbb{R}^d$, the quantum state $|\mathbf{x}\rangle = \sum_z x_z |z\rangle$. need $\log(d)$ qubits for a data point; In general, it is hard to prepare such state. (subject to dequantization [28]). typical encoding method for quantum machine learning for classical problems (such as image classification).
- **unitary encoding:** quantum simulation (Hamiltonian); quantum random walk (adjacency matrix); oracle (controlled) unitary, e.g., quantum phase estimation; **graph state** encoding (discrete, efficient in space/time?, isomorphism?)
- **quantum data:** quantum state $|\psi\rangle$ or ρ from real-world experiments or designed quantum circuits \hat{U} . no input problem? more efficient? for quantum algorithms

Question 3. *how to relate graph state entanglement to graph property test ..??.*

Definition 24 (graph property). monotone ...

Example 6 (colorable). k -colorable is a graph property, i.e., allow for a coloring of the vertices with k colors such that no two adjacent vertices have the same color. A graph is bipartite iff 2-colorable. other graph properties: isomorphism; vertex cover; Hamiltonian cycle ...

Problem 8 (graph property test). **promise:** the input graph either has a property, or is ϵ -far from having the property, meaning that we must change at least an ϵ fraction of the edges to make the property hold.

330 **Theorem 7** (bounds for graph property test).

331 **Question 4.** [29] Is there any graph property which admits an exponential quantum speed-up? [30] depends on input
332 model (query adjacency matrix/list)

333 Graphs is another kind of data which is fundamentally different from a real value vector because of vertex-edge
334 relation and graph isomorphism. So, graph kernel [31] need additional attention.

335 **Definition 25** (graph kernel). given a pair of graphs (G, G') , graph kernel is $k(G, G') =$. quantum graph kernel
336 $k(G, G') = |\langle G | G' \rangle|^2$?? [32]

337 A. Classical shadow and machine learning

338 related works

- 339 • separability classifier by classical neural network [33]: input: sythetic random density matrices; output: a
340 classical classifier for **bipartite separable** (independent of state??). The idea is to feed the classifier by a large
341 amount of sampled trial states (feature: synthetic density matrix with noise flatten as a real vector $\mathbf{x} \in \mathbb{R}^{d_A^2 d_B^2 - 1}$)
342 as well as their corresponding class labels (separable or entangled by **PPT criterion**, CHA), and then train the
343 classifier to predict the class labels of new states that it has not encountered before. Previous methods **only**
344 **detect a limited part of the state space**, e.g. different entangled states often require different **entanglement**
345 **witness**. In contrast, this classifier can handle a variety?? of input states once properly trained Fig. 1.
- 346 • Bell inequaliity and NN [23]
- 347 • SVM, (universal), 4 qubit [34]
- 348 • **classical shadow** [3]: estimate entanglment witness (fixed but unknown target state, e.g., tripartite GHZ) En-
349 tanglement verification. Fidelities with pure target states can also serve as (bipartite) entanglement witnesses.
350 For every (bipartite) entangled state ρ , there exists a constant α and an observable $\hat{O} = |\psi\rangle\langle\psi|$ such that
351 $\text{Tr}(\hat{O}\rho) > \alpha \geq \text{Tr}(\hat{O}\rho_s)$, for all (bipartite) separable states ρ_s . Establishing $\text{Tr}(\hat{O}\rho) > \alpha$ verifies the existence
352 of entanglement in the state ρ . Any $\hat{O} = |\psi\rangle\langle\psi|$ that satisfies the above condition is known as an entangle-
353 ment witness for the state ρ . **Classical shadows (Clifford measurements) of logarithmic size allow for**
354 **checking a large number of potential entanglement witnesses simultaneously**. Directly measuring M
355 different entanglement witnesses requires a number of quantum measurements that scales (at least) linearly in
356 M . In contrast, classical shadows get by with $\log(M)$ -many measurements only. classical shadows are based
357 on random Clifford measurements and do not depend on the structure of the concrete witness in question. In
358 contrast, direct estimation crucially depends on the concrete witness in question and may be considerably more
359 difficult to implement.
- 360 • classical SVM: An SVM allows for the construction of a hyperplane $\langle \hat{W} \rangle = \sum_k w_k \mathbf{x}_k$ that clearly delineates
361 between separable states and the target entangled state (bipartite and **tripartite qubit and qudit**); this
362 hyperplane is a **weighted sum of observables ('features') whose coefficients are optimized during**
363 **the training of the SVM**. This method the ability to obtain witnesses that require only local measurements
364 even when the target state is a **non-stabilizer state** W state (normally need nonlocal measurements). feature:
365 \mathbf{x}_k expectation of Pauli strings. the training of an SVM is convex; if a solution exists for the given target state
366 and ansatz, the optimal SVM 2 will be found. this SVM formalism allows for the programmatic removal of
367 features, i.e., reducing the number of experimental measurements, in exchange for a lower tolerance to white
368 noise, in a manner similar to [??].
- 369 • classical machine learning (SVM, NN) with **classical shadow** [35]?: classify phase, predict ground state, entan-
370 glement?

371 1. Classical shadow

372 Inspired by Aaronson's shadow tomography [27], Huang et. al [3] introduce classical shadow. A classical shadow is a
373 succinct classical description of a quantum state, which can be extracted by performing reasonably simple single-copy

measurements on a reasonably small number of copies of the state. The classical shadow attempts to approximate this expectation value by an empirical average over T independent samples, much like Monte Carlo sampling approximates an integral.

Definition 26 (classical shadow). classical shadow (snapshots) ρ_{cs}

$$\rho_{cs} = \mathcal{M}^{-1} \left(U^\dagger \left| \hat{b} \right\rangle \left\langle \hat{b} \right| U \right) \quad (22)$$

such that we can predict the linear function with classical shadows

$$o_i = \text{Tr}(O_i \rho_{cs}) \text{ obeys } \mathbb{E}[o] = \text{Tr}(O_i \rho) \quad (23)$$

The classical shadow size required to accurately approximate all reduced r -body density matrices scales exponentially in subsystem size r , but is independent of the total number of qubits n .

Algorithm III.1: Classical Shadow (tomography)

input : an (unknown) density matrix ρ (many copies, black-box access to a circuit preparing a state)
output: classical shadow ρ_{cs}

```

1 for  $i = 1, 2, \dots, N$  do
2    $\rho \mapsto \hat{U} \rho \hat{U}^\dagger$  // apply a random unitary to rotate the state
3    $\mapsto |b\rangle \dots$  // perform a computational-basis measurement
4    $\rho_{cs} = \mathcal{M}^{-1} \left( \hat{U}^\dagger |b\rangle \langle b| \hat{U} \right)$  // measurement outcome  $|b\rangle \in \{0, 1\}^n$ ,  $\mathcal{M}$  quantum channel
5 return  $S(\rho, N) = \left\{ \rho_{cs_1} = \mathcal{M}^{-1} \left( \hat{U}_1^\dagger |b_1\rangle \langle b_1| \hat{U}_1 \right), \dots, \rho_{cs_N} \right\}$  // call this array the classical shadow of  $\rho$ 
```

A classical shadow is created by repeatedly performing a simple procedure: Apply a unitary transformation $\rho \mapsto \hat{U} \rho \hat{U}^\dagger$, and then measure all the qubits in the computational basis. The number of times this procedure is repeated is called the size of the classical shadow. The transformation U is randomly selected from an ensemble of unitaries, and different ensembles lead to different versions of the procedure that have characteristic strengths and weaknesses. Classical shadows with size of order $\log(M)$ suffice to predict M target functions $\{\hat{O}_1, \dots, \hat{O}_M\}$.

Lemma 1. *predict linear function with shadow shadow: the variance*

$$\text{Var}[o] = \mathbb{E}[(o - \mathbb{E}[o])^2] \leq \left\| O - \frac{\text{Tr}(O)}{2^n} \mathbb{1} \right\|_{\text{shadow}}^2 \quad (24)$$

Theorem 8. *Fix a measurement primitive $\mathcal{U}??$, a collection $\{\hat{O}_1, \dots, \hat{O}_M\}$ of $2^n \times 2^n$ Hermitian matrices and accuracy parameters $\epsilon, \delta \in [0, 1]$. Set*

$$K = 2 \log(2M/\delta), \quad N = \frac{34}{\epsilon^2} \max_{1 \leq i \leq M} \left\| \hat{O}_i - \frac{\text{Tr}(O_i)}{2^n} \mathbb{1} \right\|_{\text{shadow}}^2 \quad (25)$$

where $\|\cdot\|_{\text{shadow}}$ is shadow norm. Then, a collection of NK independent classical shadows allow for accurately predicting all features via median of means prediction

$$|o_i(N, K) - \text{Tr}(O_i \rho)| \leq \epsilon, \quad \forall i \leq M \quad (26)$$

with probability at least $1 - \delta$. $o_i(N, K) = \text{median} \left\{ \text{Tr}(\hat{O}_i \rho_{(1)}), \dots, \text{Tr}(\hat{O}_i \rho_{(K)}) \right\}$

Definition 27 (shadow norm). $\|\cdot\|_{\text{shadow}}$ is shadow norm that only depends on the measurement primitive:

$$\|O\|_{\text{shadow}} = \max_{\sigma: \text{state}} \left(\mathbb{E}_{U \sim \mathcal{U}} \sum_{b \in \{0, 1\}^n} \langle b | \hat{U} \sigma \hat{U}^\dagger | b \rangle \langle b | \hat{U} \mathcal{M}^{-1}(O) \hat{U}^\dagger | b \rangle^2 \right)^{1/2} \quad (27)$$

(nonnegative, homogeneous, triangle inequality)

Theorem 9 (Pauli/Clifford measurements). *Any procedure based on a fixed set of single-copy local measurements that can predict, with additive error ϵ , M arbitrary k -local linear function $\text{Tr}(\hat{O}_i \rho)$, requires at least (lower bound) $\Omega(\log(M)3^k/\epsilon^2)$ copies of the state ρ . $\Omega(\log(M) \max_i \text{Tr}(\hat{O}_i^2)/\epsilon^2)$*

Consider a simple family of entanglement witnesses with compatible structure: (ansatz??)

$$O := O(V_A, V_B, V_C) = V_A \otimes V_B \otimes V_C |\psi_{\text{GHZ}}^+\rangle\langle\psi_{\text{GHZ}}^+| V_A^\dagger \otimes V_B^\dagger \otimes V_C^\dagger \quad (28)$$

the single-qubit unitaries V_A, V_B, V_C parametrize different witnesses. for any state ρ_s with only bipartite entanglement, $\text{Tr}(\hat{O}_{\rho_s}) \leq 0.5$, while for any state ρ_s with at most W -type entanglement, $\text{Tr}(\hat{O}_{\rho_s}) \leq 0.75$. Therefore verifying that $\text{Tr}(\hat{O}_{\rho}) \geq 0.5$ certifies that ρ has tripartite entanglement, while $\text{Tr}(\hat{O}_{\rho}) > 0.75$ certifies that ρ has GHZ-type entanglement.

2. Derandomization

Derandomization can and should be viewed as a refinement of the original classical shadows idea. [36] [37]

3. training data and classical kernel methods

$\sigma_T(\rho(x_l))$ is the classical shadow representation of $\rho(x_l)$, a $2^n \times 2^n$ matrix that reproduces $\rho(x_l)$ in expectation over random Pauli measurements.

$$\{x_l \rightarrow \sigma_T(\rho(x_l))\}_{l=1}^N \quad (29)$$

Definition 28 (shadow kernel). given two density matrices (quantum states) ρ and ρ' , *shadow kernel* [3] is

$$k_{\text{shadow}}(S_T(\rho), S'_T(\rho')) := \exp\left(\frac{\tau}{T^2} \sum_{t,t'=1}^T \exp\left(\frac{\gamma}{n} \sum_{i=1}^n \text{Tr}(\sigma_i^{(t)} \sigma_i^{(t')})\right)\right) \quad (30)$$

where $S_T(\rho)$ is the classical shadow representation of ρ . The computation time for the inner product is $\mathcal{O}(nT^2)$, linear in the system size n and quadratic in T , the number of copies of each quantum state which are measured to construct the classical shadow.

Proposition 7 ([4]). *exist quantum advantage in machine learning (not significant, practical) ... discrete log, factoring...*

Algorithm III.2: Classical learning (SVM) + classical shadow

input : classical shadow? (features) with label (training data); ansatz $\hat{W}_{\text{ml}} = \mathbf{w} \cdot \vec{\sigma}$

output: entanglement structure? decision separable; classify phase

// ----- training phase -----

1 **for** $i = 1, 2, \dots, m$ **do**

2 kernel estimation // classical kernel

3 SVM // SVM

4 **return** \mathbf{w} // parameters of the separating hyperplane in the feature space

// ===== testing phase ===== //

5 **return** $\mathbf{w} \cdot \vec{\sigma} < 0$: separable // predict

B. Quantum trace (kernel) estimation

1. Entanglement spectroscopy via quantum trace estimation

For $\text{Tr}(\rho_A^m)$, an important application of multivariate trace estimation [5] is to entanglement spectroscopy [38] [39] [37] - deducing the full set of eigenvalues of ρ_A . The smallest eigenvalue of diagnoses whether ψ_{AB} is separable or

entangled [40]. The well-known identity (related to the replica trick originating in spin glass theory)

$$\text{Tr}(\hat{U}^\pi(\rho_1 \otimes \cdots \otimes \rho_m)) = \text{Tr}(\rho_1 \cdots \rho_m) \quad (31)$$

where the RHS is the multivariate trace and \hat{U}^π is a unitary representation of the cyclic shift permutation. While the left-hand-side is ... We can estimate the quantities $\text{Re}[\text{Tr}(\rho_1 \cdots \rho_m)]$ and $\text{Im}[\text{Tr}(\rho_1 \cdots \rho_m)]$ respectively. to generalize the estimation beyond single-qubit states, we can either increase the width or the depth of the circuit described above.

Remark 10 ([40]). Direct entanglement detections, can be **employed as sub-routines in quantum computation**. For example, one may consider performing or not performing a quantum operation on a given quantum system conditioned on some part of quantum data being entangled or not. In fact direct entanglement detections can be viewed as quantum computations solving an inherently quantum decision problem: given as an input n copies of decide whether is entangled. Here the **input data is quantum** and such a decision problem cannot even be even formulated for classical computers.

For the sake of completeness we should also mention here that there are two-particle observables, called entanglement witnesses which can detect quantum entanglement in some special cases (see [20,8]). They have positive mean values on all separable states and negative on some entangled states. Therefore **any individual entanglement witness leaves many entangled states undetected**. When is unknown we need to check infinitely many witnesses, which effectively reduces this approach to the quantum state estimation. However, let us point out any witness defines a positive map which can be used in our test.

Definition 29 (entanglement spectroscopy). the concept of the entanglement spectrum which is the energy spectrum of the “entanglement Hamiltonian” \hat{H}_E defined through $\rho_A = \exp(\hat{H}_E)$. They pointed out that the largest eigenvalues of ρ_A [30] contain more universal signatures than the von Neumann entropy or S_2 alone. (SWAP trick, Quantum phase estimation) [39]:

Theorem 10 ([5]). *multivariate trace estimation can be implemented in **constant depth**, with only linearly-many controlled two-qubit gates and a linear amount of classical pre-processing. copies $\mathcal{O}(\epsilon^{-2} \log(\delta^{-1}))$...*

Theorem 11. *Let $\{\rho_1, \dots, \rho_m\}$ be a set of p -qubit states, and fix $\epsilon > 0$ and $\delta \in (0, 1)$. There exists a random variable \hat{T}_p that can be computed using $\mathcal{O}(\mathcal{O}(\epsilon^{-2} \log(\delta^{-1})))$ repetitions of a **constant-depth** quantum circuit consisting of $\mathcal{O}(mp)$ three-qubit gates, and satisfies*

$$\mathbb{P}\left(\left|\hat{T}_p - \text{Tr}(\rho_1 \cdots \rho_m)\right| \leq \epsilon\right) \geq 1 - \delta. \quad (32)$$

Algorithm III.3: entanglement spectroscopy by ... quantum trace estimation

input : (copies of) density matrix (graph state?) ρ, \dots
output: spectrum of entanglement Hamiltonian

```

1 for  $i = 1, 2, \dots, m$  do
2   GHZ // prepare GHZ
3   parallel // estimate real and imaginary part respectively
4   return  $\lambda$ 
5 return smallest eigenvalue of  $\rho_A$ 

```

Remark 11 ([5]). We remark that, an alternative way to estimate $\text{Tr}[\rho^k]$ for each $k \in [m]$ is by using the method of classical shadows to obtain ‘classical snapshots’ of ρ that can be linearly combined to obtain a classical random variable whose expectation is $\text{Tr}[\rho^k]$ (see Supplementary Material Section 6 of [3]). However, it is **unclear to us if this method would offer savings in the quantum resources required, as the total number of times the quantum circuit needs to be run in the data acquisition phase should scale with the variance of the corresponding estimator**. We do not know of a concise expression for this variance for arbitrary m . Indeed, calculating it for just a single value of m ($m = 2$) required four pages of calculations in [3].

2. Estimate entanglement witness by quantum machine learning

The quantum ML algorithm accesses the quantum channel \mathcal{E}_ρ multiple times to obtain multiple copies of the underlying quantum state ρ . Each access to \mathcal{E}_ρ allows us to obtain one copy of ρ . Then, the quantum ML algo-

455 rithm performs a sequence of measurements on the copies of ρ to accurately predict $\text{Tr}(P_x \rho), \forall x \in \{I, X, Y, Z\}^n$.

Algorithm III.4: [entanglement witness](#) by quantum ML

input : (copies of) density matrix ρ , an entanglement witness (observable) \hat{W}
output: $\text{Tr}(P_x \rho), \forall x \in \{I, X, Y, Z\}^n$

```

456 1 for  $i = 1, 2, \dots, m$  do
457   2  $\perp P_x$  // estimate entanglement witness by quantum ML
458 3 return estimation of  $\text{Tr}(\hat{W}\rho)$ 

```

457 **Theorem 12** ([41]). For M Pauli opertors, there is a (quantum) procedure estimate every expectation value
458 $\text{Tr}(P_x \rho), \forall i = 1, \dots, M$ within error ϵ under probability at least $1 - \delta$ by performing POVM measurements on
459 $\mathcal{O}(\log(M/\delta)\epsilon^{-4})$ copies of the unknown quantum state ρ . ($M = 4^n$ implies linear copy for full tomography???)

460 **Theorem 13** ([41]). We rigorously show that, for any quantum process \mathcal{E} , observables \hat{O} , and distribution \mathcal{D} , and
461 for any quantum ML model, one can always design a classical ML model achieving a similar average prediction error
462 such that N_C (number of experiments?) is larger than N_Q by at worst a small polynomial factor.

463 In contrast, for achieving accurate prediction on all inputs, we prove that **exponential quantum advantage is**
464 **possible**. For example, to predict expectations of all **Pauli observables** (entanglement witness??) in an n -qubit
465 system ρ , classical ML models require $2^{\Omega(n)}$ copies of ρ , but we present a quantum ML model using only $\mathcal{O}(n)$ copies.

466 3. Quantum kernel SVM

467 related works:

- 468 • quantum kernel method: estimate kernels by quantum algorithms (circuits) [42] [43]: for classical problem (data)
- 469 • rigorous and robust quantum advantage of quantum kernel method in SVM [44]. group structured data [45]
- 470 • power of data in quantum machine learning [4]: input??? projected quantum kernel

471 **Definition 30** (quantum kernel). quantum kernel with quantum feature map $\phi(\mathbf{x}) : \mathcal{X} \rightarrow |\phi(\mathbf{x})\rangle\langle\phi(\mathbf{x})|$

$$k_Q(\rho, \rho') := |\langle\phi(\mathbf{x})|\phi(\mathbf{x}')\rangle|^2 = \left| \langle 0 | \hat{U}_{\phi(\mathbf{x})}^\dagger \hat{U}_{\phi(\mathbf{x}')} | 0 \rangle \right|^2 = \text{Tr}(\rho \rho') \equiv \langle \rho, \rho' \rangle_{\text{HS}} \quad (33)$$

472 where $\hat{U}_{\phi(\mathbf{x})}$ is a quantum circuit or physics process that encoding an input \mathbf{x} . In quantum physics, quantum kernel
473 is also known as transition amplitude (quantum propagator);

474 **Proposition 8** ([4]). If a classical algorithm without training data can compute (label) $y = f(x) = \langle x | \hat{U}_{\text{QNN}}^\dagger \hat{O} U_{\text{QNN}} | x \rangle$
475 (with amplitude encoding) efficiently (poly time in ...) for any \hat{U}_{QNN} and \hat{O} , then **BPP** = **BQP** (which is believed
476 unlikely).

477 **Proposition 9** ([4]). Training an arbitrarily deep quantum neural network \hat{U}_{QNN} with a trainable observable \hat{O} is
478 equivalent to training a [quantum kernel](#) method with kernel $k_Q(\mathbf{x}, \mathbf{x}') = \text{Tr}(\rho(\mathbf{x})\rho'(\mathbf{x}'))$

479 **Definition 31** (projected quantum kernel).

480 C. Variational (hybrid) quantum algorithms

481 1. Variational entanglement witness (ansatz)

482 an ansatz for [entanglement witness](#) [21] (graph state entanglement)

$$\hat{W}_{\text{ansatz}} := \sum_{\mathbf{p} \in \{I, X, Y, Z\}^n} w_{\mathbf{p}} \bigotimes_i^n \hat{\sigma}^{(\mathbf{p}_i)} \quad (34)$$

483 c.f. [full tomography](#) (Stokes parameters) Eq. (21)

Algorithm III.5: ansatz + classical shadow (quantum ML) + classical SVM

input : (copies of) ρ , an entanglement witness (observable); ansatz $\hat{W}_{\text{ml}} = \mathbf{w} \cdot \vec{\sigma}$
output: classifier \mathbf{w}

```

484 1 for  $i = 1, 2, \dots, m$  do
2   |  $\rho_{cs}$                                      // classical shadow
3   |  $\mathbf{w} \mathbf{x}$                                // optimize SVM
4 return parameters  $\mathbf{w}$  (SVM hyperplane)

```

Theorem 14. *On quantum computers, evaluating the trace distances is probably hard since even judging whether ρ and ρ' have large or small trace distance is known to be QSZK-complete [46], where QSZK (quantum statistical zero-knowledge) is a complexity class that includes BQP (bounded-error quantum polynomial time). [47]*

D. Theoretic upper bounds and lower bounds

[3] [41] [4] [27]

	gate/depth/computation	measurements/samples	query?	input/unknown?
shadow tomography	exp circuit?	Theorem 6	N/A	unknown
entanglement witness	N/A	Proposition 6 (constant?)	convex?[48]	known
classical shadow	N/A	Theorems 8 and 9	N/A	unknown?
C. ML + C. entanglement witness ansatz	??	Q. advantage Theorem 13	N/A	unknown
QML. entanglement witness ansatz	??	Theorem 12	N/A	unknown
Q. entanglement spectroscopy	Theorem 10 (c-depth?)		property test [29]	unknown
SVM + quantum kernel estimation				??

TABLE II: complexity (different measures) of different methods

	circuits	number of copies (measurements)
classical shadow		
derandomized		
quantum circuit		

TABLE III: trace estimation

	observables	weights	input
entanglement witness			known
Bell (CHSH) inequality		unknown	
entangle **spectrum??		unknown	

TABLE IV: ansatz

	accuracy	complexity
linear SVM		
kernel SVM		
Neural network		
neural kernel		
quantum kernel		

TABLE V: machine learning methods

1. Separations (complexity)

contrived problem (engineered dataset)? for exponential speedup

2. Obstacles (practical)

IV. NUMERICAL SIMULATION

A. Classification accuracy

1. Data preparation

multi-partite entangled state: generate synthetic (engineered) data from (random graph?). separable state from randomly ...

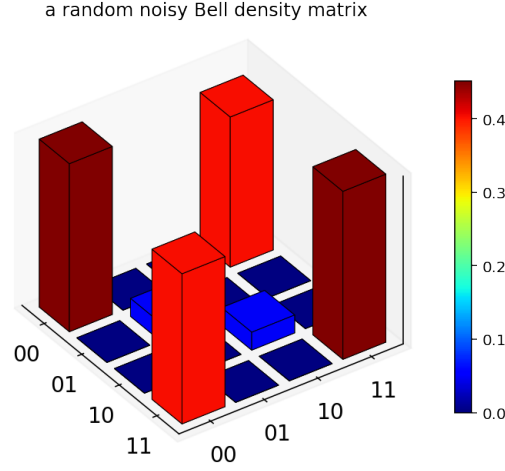


FIG. 3: Bell state with white noise

2. Hyperparameters and settings

We consider a set of different regularization parameters,...

3. Results

performance of different methods:

FIG. 4: comparison of

B. Robustness to noise

tradeoff between (white noise) tolerance (robustness) and efficiency (number of measurements).

$$\rho'_{\text{noise}} = (1 - p_{\text{noise}}) |G\rangle\langle G| + p_{\text{noise}} \frac{\mathbb{1}}{2^n} \quad (35)$$

p_{noise} indicates the robustness of the algorithm (witness).

Remark 12 ([2]). the largest noise tolerance p_{limit} just related to the **chromatic number** (graph property) of the graph.

Question 5. other noise (depolarization)? e.g., flip error, phase error?, local, random unitary transformation?

find optimal (robustness) entanglement witness by classical machine learning (qunatum circuit?)

FIG. 5: robustness

C. Experiments

future: experimental (photonic) implementation with a few qubits (generation, verification) [49]

V. CONCLUSION AND DISCUSSION

Acknowledgements

-
- [1] R. Horodecki, P. Horodecki, M. Horodecki, and K. Horodecki, *Rev. Mod. Phys.* **81**, 865 (2009), [arXiv:quant-ph/0702225](#).
 - [2] Y. Zhou, Q. Zhao, X. Yuan, and X. Ma, *npj Quantum Inf* **5**, 83 (2019).
 - [3] H.-Y. Huang, R. Kueng, and J. Preskill, *Nat. Phys.* **16**, 1050 (2020), [arXiv:2002.08953 \[quant-ph\]](#).
 - [4] H.-Y. Huang, M. Broughton, M. Mohseni, R. Babbush, S. Boixo, H. Neven, and J. R. McClean, *Nat Commun* **12**, 2631 (2021), [arXiv:2011.01938 \[quant-ph\]](#).
 - [5] Y. Quek, M. M. Wilde, and E. Kaur, *Multivariate trace estimation in constant quantum depth* (2022), [arXiv:2206.15405 \[hep-th, physics:quant-ph\]](#).
 - [6] C. Bădescu, R. O'Donnell, and J. Wright, *Quantum state certification* (2017), [arXiv:1708.06002 \[quant-ph\]](#).
 - [7] L. Gurvits, *Classical deterministic complexity of Edmonds' problem and Quantum Entanglement* (2003), [arXiv:quant-ph/0303055](#).
 - [8] L. M. Ioannou, *Quantum Inf. Comput.* **7**, 335 (2007), [arXiv:quant-ph/0603199](#).
 - [9] M. Horodecki, P. Horodecki, and R. Horodecki, *Physics Letters A* **223**, 1 (1996), [arXiv:quant-ph/9605038](#).
 - [10] H. J. Briegel, D. E. Browne, W. Dür, R. Raussendorf, and M. V. den Nest, *Nature Phys* **5**, 19 (2009), [arXiv:0910.1116](#).
 - [11] M. Hein, W. Dür, J. Eisert, R. Raussendorf, M. V. den Nest, and H.-J. Briegel, *Entanglement in Graph States and its Applications* (2006), [arXiv:quant-ph/0602096](#).
 - [12] Y. Zhang, Y. Tang, Y. Zhou, and X. Ma, *Phys. Rev. A* **103**, 052426 (2021), [arXiv:2012.07606 \[quant-ph\]](#).
 - [13] X. Gao and L.-M. Duan, *Nat Commun* **8**, 662 (2017), [arXiv:1701.05039 \[cond-mat, physics:quant-ph\]](#).
 - [14] C. de Gois, K. Hansenne, and O. Gühne, *Uncertainty relations from graph theory* (2022), [arXiv:2207.02197 \[quant-ph\]](#).
 - [15] O. Gühne and G. Toth, *Physics Reports* **474**, 1 (2009), [arXiv:0811.2803 \[cond-mat, physics:physics, physics:quant-ph\]](#).
 - [16] B. M. Terhal, *Physics Letters A* **271**, 319 (2000), [arXiv:quant-ph/9911057](#).
 - [17] T. Heinosaari and M. Ziman, *The Mathematical Language of Quantum Theory: From Uncertainty to Entanglement*, 1st ed. (Cambridge University Press, 2011).
 - [18] G. Toth and O. Guehne, *Phys. Rev. Lett.* **94**, 060501 (2005), [arXiv:quant-ph/0405165](#).
 - [19] G. Tóth and O. Gühne, *Phys. Rev. A* **72**, 022340 (2005).
 - [20] O. Gühne and N. Lütkenhaus, *Phys. Rev. Lett.* **96**, 170502 (2006).
 - [21] E. Y. Zhu, L. T. H. Wu, O. Levi, and L. Qian, *Machine Learning-Derived Entanglement Witnesses* (2021), [arXiv:2107.02301 \[quant-ph\]](#).
 - [22] M. Bourennane, M. Eibl, C. Kurtsiefer, S. Gaertner, H. Weinfurter, O. Guehne, P. Hyllus, D. Bruss, M. Lewenstein, and A. Sanpera, *Phys. Rev. Lett.* **92**, 087902 (2004), [arXiv:quant-ph/0309043](#).
 - [23] Y.-C. Ma and M.-H. Yung, *npj Quantum Inf* **4**, 34 (2018), [arXiv:1705.00813 \[quant-ph\]](#).
 - [24] S. Sciara, C. Reimer, M. Kues, P. Roztock, A. Cino, D. J. Moss, L. Caspani, W. J. Munro, and R. Morandotti, *Phys. Rev. Lett.* **122**, 120501 (2019).
 - [25] J. Altepeter, E. Jeffrey, and P. Kwiat, in *Advances In Atomic, Molecular, and Optical Physics*, Vol. 52 (Elsevier, 2005) pp. 105–159.
 - [26] J. Haah, A. W. Harrow, Z. Ji, X. Wu, and N. Yu, *IEEE Trans. Inform. Theory*, 1 (2017).
 - [27] S. Aaronson, in *Proceedings of the 50th Annual ACM SIGACT Symposium on Theory of Computing*, STOC 2018 (Association for Computing Machinery, New York, NY, USA, 2018) pp. 325–338, [arXiv:1711.01053](#).
 - [28] E. Tang, *Phys. Rev. Lett.* **127**, 060503 (2021), [arXiv:1811.00414 \[quant-ph\]](#).
 - [29] A. Montanaro and R. de Wolf, *A Survey of Quantum Property Testing* (2018), [arXiv:1310.2035 \[quant-ph\]](#).
 - [30] S. Ben-David, A. M. Childs, A. Gilyén, W. Kretschmer, S. Podder, and D. Wang, *2020 IEEE 61st Annu. Symp. Found. Comput. Sci. FOCS*, 649 (2020), [arXiv:2006.12760](#).
 - [31] N. M. Kriege, F. D. Johansson, and C. Morris, *Appl Netw Sci* **5**, 6 (2020), [arXiv:1903.11835 \[cs, stat\]](#).
 - [32] L. Bai, L. Rossi, A. Torsello, and E. R. Hancock, *Pattern Recognition* **48**, 344 (2015).
 - [33] S. Lu, S. Huang, K. Li, J. Li, J. Chen, D. Lu, Z. Ji, Y. Shen, D. Zhou, and B. Zeng, *Phys. Rev. A* **98**, 012315 (2018), [arXiv:1705.01523 \[quant-ph\]](#).

- [34] S. V. Vintskevich, N. Bao, A. Nomerotski, P. Stankus, and D. A. Grigoriev, [Classification of four-qubit entangled states via Machine Learning](#) (2022), [arXiv:2205.11512 \[quant-ph\]](#).
- [35] H.-Y. Huang, R. Kueng, G. Torlai, V. V. Albert, and J. Preskill, [Provably efficient machine learning for quantum many-body problems](#) (2021), [arXiv:2106.12627 \[quant-ph\]](#).
- [36] H.-Y. Huang, R. Kueng, and J. Preskill, [Phys. Rev. Lett.](#) **127**, 030503 (2021), [arXiv:2103.07510 \[quant-ph\]](#).
- [37] A. Elben, R. Kueng, H.-Y. Huang, R. van Bijnen, C. Kokail, M. Dalmonte, P. Calabrese, B. Kraus, J. Preskill, P. Zoller, and B. Vermersch, [Phys. Rev. Lett.](#) **125**, 200501 (2020), [arXiv:2007.06305 \[cond-mat, physics:quant-ph\]](#).
- [38] A. K. Ekert, C. M. Alves, D. K. L. Oi, M. Horodecki, P. Horodecki, and L. C. Kwek, [Phys. Rev. Lett.](#) **88**, 217901 (2002), [arXiv:quant-ph/0203016](#).
- [39] S. Johri, D. S. Steiger, and M. Troyer, [Phys. Rev. B](#) **96**, 195136 (2017), [arXiv:1707.07658](#).
- [40] P. Horodecki and A. Ekert, [Phys. Rev. Lett.](#) **89**, 127902 (2002), [arXiv:quant-ph/0111064](#).
- [41] H.-Y. Huang, R. Kueng, and J. Preskill, [Phys. Rev. Lett.](#) **126**, 190505 (2021), [arXiv:2101.02464 \[quant-ph\]](#).
- [42] V. Havlicek, A. D. Córcoles, K. Temme, A. W. Harrow, A. Kandala, J. M. Chow, and J. M. Gambetta, [Nature](#) **567**, 209 (2019), [arXiv:1804.11326](#).
- [43] M. Schuld and N. Killoran, [Phys. Rev. Lett.](#) **122**, 040504 (2019), [arXiv:1803.07128 \[quant-ph\]](#).
- [44] Y. Liu, S. Arunachalam, and K. Temme, [Nat. Phys.](#) **17**, 1013 (2021), [arXiv:2010.02174 \[quant-ph\]](#).
- [45] J. R. Glick, T. P. Gujarati, A. D. Corcoles, Y. Kim, A. Kandala, J. M. Gambetta, and K. Temme, [Covariant quantum kernels for data with group structure](#) (2021), [arXiv:2105.03406 \[quant-ph\]](#).
- [46] J. Watrous, [Quantum Computational Complexity](#) (2008), [arXiv:0804.3401 \[quant-ph\]](#).
- [47] R. Chen, Z. Song, X. Zhao, and X. Wang, [Quantum Sci. Technol.](#) **7**, 015019 (2022), [arXiv:2012.05768 \[math-ph, physics:quant-ph\]](#).
- [48] S. Chakrabarti, A. M. Childs, T. Li, and X. Wu, [Quantum](#) **4**, 221 (2020), [arXiv:1809.01731 \[quant-ph\]](#).
- [49] H. Lu, Q. Zhao, Z.-D. Li, X.-F. Yin, X. Yuan, J.-C. Hung, L.-K. Chen, L. Li, N.-L. Liu, C.-Z. Peng, Y.-C. Liang, X. Ma, Y.-A. Chen, and J.-W. Pan, [Phys. Rev. X](#) **8**, 021072 (2018).
- [50] A. Jacot, F. Gabriel, and C. Hongler, [Neural Tangent Kernel: Convergence and Generalization in Neural Networks](#) (2020), [arXiv:1806.07572 \[cs, math, stat\]](#).

Appendix A: Machine learning background

Notations: The (classical) training data (for supervised learning) is a set of m data points $\{(\mathbf{x}^{(i)}, y^{(i)})\}_{i=1}^m$ where each data point is a pair (\mathbf{x}, y) . Normally, the input (e.g., an image) $\mathbf{x} := (x_1, x_2, \dots, x_d) \in \mathbb{R}^d$ is a vector where d is the number of *features* and its *label* $y \in \Sigma$ is a scalar with some discrete set Σ of alphabet/categories. For simplicity and the purpose of this paper, we assume $\Sigma = \{-1, 1\}$ (binary classification).

1. Support vector machine

Definition 32 (SVM). Given a set of (binary) labeled data, support vector machine (SVM) is designed to find a hyperplane (a linear function) such that maximize the margin between two partitions...

$$\max_{\mathbf{w}} \dots \quad (\text{A1})$$

a. kernel method

nonlinear boundary. map to a higher dimensional (feature) space, in which data is linearly separable. [kernel](#)

Definition 33 (kernel). In general, the kernel function $k : \mathcal{X} \times \mathcal{X} \rightarrow \mathbb{R}$ measures the similarity between two input data points by an inner product

$$k(\mathbf{x}, \mathbf{x}') := \langle \phi(\mathbf{x}), \phi(\mathbf{x}') \rangle \quad (\text{A2})$$

If the input $\mathbf{x} \in \mathbb{R}^d$ (conventional machine learning task, e.g., image classification), the feature map $\phi(\mathbf{x}) : \mathbb{R}^d \rightarrow \mathbb{R}^n$ ($d < n$) from a low dimensional space to a higher dimensional space. The corresponding kernel (Gram) matrix \mathbf{K} should be a positive, semidefinite (PSD) matrix, i.e. all eigenvalues are non-negative

Example 7 (kernels). Some common kernels: the polynomial kernel $k_{\text{poly}}(\mathbf{x}, \mathbf{x}') := (1 + \mathbf{x} \cdot \mathbf{x}')^q$ with feature map $\phi(\mathbf{x}) \dots$ The Gaussian kernel $k_{\text{gaus}}(\mathbf{x}, \mathbf{x}') := \exp\left(-\gamma \|\mathbf{x} - \mathbf{x}'\|_2^2\right)$ with an infinite dimensional feature map $\phi(\mathbf{x})$. An important feature of kernel method is that kernels can be computed efficiently without evaluating feature map (might be infinite dimension) explicitly.

607 similarity measures? advantages? why? (isomorphism?)

608 **Definition 34** (divergence). KL divergence (relative [entropy](#)): measure the distance (similarity) between two prob-
609 ability distributions:

$$D_{\text{KL}}(P||Q) := \sum P(x) \log(P(x)/Q(x)) \quad (\text{A3})$$

610 symmetric version: Jensen-Shannon divergence (machine learning)

$$D_{\text{JS}}(P||P') := \frac{1}{2}(D_{\text{KL}}(P||M) + D_{\text{KL}}(P'||M)) \equiv H_S(M) - \frac{1}{2}(H_S(P) + H_S(P')) \quad (\text{A4})$$

611 where $M = (P + P')/2$ and Shannon [entropy](#) H_S . Analogously, quantum Jensen-Shannon divergence D_{QJS} of two
612 density matrices can be defined...

$$D_{\text{QJS}}(\rho||\rho') := H_V(\rho_M) - \frac{1}{2}(H_V(\rho) + H_V(\rho')) \quad (\text{A5})$$

613 as a quantum graph kernel (ρ induced by quantum random walk)

Definition 35 (geometric difference).

$$g(K^1||K^2) = \sqrt{\left\| \sqrt{K^2}(K^1)^{-1}\sqrt{K^2} \right\|_{\infty}} \quad (\text{A6})$$

614 where $\|\cdot\|_{\infty}$ is the spectral [norm](#).

615 2. Neural network

616 a. neural network and kernel

617 **Definition 36** (neural tangent kernel). neural tangent kernel [\[50\]](#): proved to be equivalent to deep neural network [\[13\]](#)
618 in the limit ...

$$k_{\text{NT}}(S_T(\rho_l), \tilde{S}_T(\rho_{l'})) = \left\langle \phi^{(\text{NT})}(S_T(\rho_l)), \phi^{(\text{NT})}(\tilde{S}_T(\rho_{l'})) \right\rangle \quad (\text{A7})$$

619 b. Stabilizer formalism

620 denote a group by \mathbb{G} and a subgroup \mathbb{H} .

621 **Definition 37** (Pauli group).

622 **Definition 38** (Clifford group).

623 **Definition 39** (Stabilizer). An observable S_k is a stabilizing operator of an n -qubit state $|\psi\rangle$ if the state $|\psi\rangle$ is an
624 eigenstate of S_k with eigenvalue 1,

625 A stabilizer set $S = \{S_1, \dots, S_n\}$ consisting of n mutually commuting and independent stabilizer operators is called
626 the set of stabilizer “generators”.

627 Many highly entangled n -qubit states can be uniquely defined by n stabilizing operators which are locally measur-
628 able, i.e., they are products of Pauli matrices. A stabilizer S_i is an n -fold tensor product of n operators chosen from
629 the one qubit Pauli operators $\{\mathbb{1}, X, Y, Z\}$.

630 c. quantum neural network

631 Appendix B: Hardness assumptions

632 **Definition 40** (NP). NP, NP-hard, NP-complete

⁶³³ **Definition 41** ($\#P$). $\#P$

⁶³⁴ **Definition 42** (QMA). QMA

⁶³⁵ **Definition 43** (BPP). BPP

⁶³⁶ **Definition 44** (BQP). BQP